

# Chiral effective field theory predictions for muon capture on deuteron and $^3\text{He}$

L.E. Marcucci<sup>a,b</sup>, A. Kievsky<sup>b</sup>, S. Rosati<sup>a</sup>, R. Schiavilla<sup>c,d</sup>, and M. Viviani<sup>b</sup>

<sup>a</sup>*Department of Physics, University of Pisa, 56127 Pisa, Italy*

<sup>b</sup>*INFN-Pisa, 56127 Pisa, Italy*

<sup>c</sup>*Department of Physics, Old Dominion University, Norfolk, VA 23529, USA*

<sup>d</sup>*Jefferson Lab, Newport News, VA 23606*

(Dated: June 5, 2021)

The muon-capture reactions  $^2\text{H}(\mu^-, \nu_\mu)nn$  and  $^3\text{He}(\mu^-, \nu_\mu)^3\text{H}$  are studied with nuclear potentials and charge-changing weak currents, derived in chiral effective field theory. The low-energy constants (LEC's)  $c_D$  and  $c_E$ , present in the three-nucleon potential and ( $c_D$ ) axial-vector current, are constrained to reproduce the  $A = 3$  binding energies and the triton Gamow-Teller matrix element. The vector weak current is related to the isovector component of the electromagnetic current via the conserved-vector-current constraint, and the two LEC's entering the contact terms in the latter are constrained to reproduce the  $A = 3$  magnetic moments. The muon capture rates on deuteron and  $^3\text{He}$  are predicted to be  $399 \pm 3 \text{ sec}^{-1}$  and  $1494 \pm 21 \text{ sec}^{-1}$ , respectively. The spread accounts for the cutoff sensitivity as well as uncertainties in the LEC's and electroweak radiative corrections. By comparing the calculated and precisely measured rates on  $^3\text{He}$ , a value for the induced pseudoscalar form factor is obtained in good agreement with the chiral perturbation theory prediction.

PACS numbers: 23.40.-s, 21.45.-v, 27.10.+h

When negative muons pass through matter, they can be captured into high-lying atomic orbitals. They then quickly cascade down into the  $1S$  orbit, where two competing processes occur: one is ordinary decay  $\mu^- \rightarrow e^- \bar{\nu}_e \nu_\mu$ , and the other is (weak) capture by the nucleus  $\mu^- A(Z, N) \rightarrow \nu_\mu A(Z-1, N+1)$ . Apart from tiny corrections due to bound-state effects (chief among which is time-dilation) [1], the decay rate is essentially the same as for a free muon and, in light nuclei, is much larger than the rate for capture. The latter proceeds predominantly through the basic process  $p\mu^- \rightarrow n\nu_\mu$  induced by the exchange of a  $W^+$  boson, and its rate, which would naively be expected to scale with the number  $Z$  of protons in the nucleus, is enhanced by an additional flux factor of  $Z^3$ , originating from the square of the atomic wave function (w.f.) evaluated at the origin [2]. Thus capture, with a rate proportional to  $Z^4$ , dominates decay at large  $Z$ .

Muon capture on hydrogen is, in principle, best suited to obtain information on the nucleon matrix element of the charge-changing quark current  $\bar{d}\gamma^\mu(1-\gamma_5)u$ , responsible for the process  $p\mu^- \rightarrow n\nu_\mu$ . Ignoring contributions from second-class currents [3] for which there is presently no firm experimental evidence [4], it is parametrized in terms of four form factors (f.f.'s): two,  $F_1(q^2)$  and  $F_2(q^2)$ , from the polar-vector component of the weak current are related to the (isovector) electromagnetic (EM) form factors of the nucleon by the conserved-vector-current (CVC) constraint; two, the axial and induced pseudoscalar f.f.'s  $G_A(q^2)$  and  $G_{PS}(q^2)$ , go along with the axial-vector part of the weak current. The  $F_1(q^2)$  and  $F_2(q^2)$  f.f.'s are well known over a wide range of momentum transfers  $q^2$  from elastic electron scattering data on the nucleon [5]. The f.f.  $G_A(q^2)$  is also quite well known: its value at vanishing  $q^2$ ,  $g_A = 1.2695(29)$ , is from neu-

tron  $\beta$ -decay [6], while its  $q^2$ -dependence is parametrized as  $G_A(q^2) = g_A/(1 - q^2/\Lambda_A^2)^2$ , with  $\Lambda_A = 1 \text{ GeV}$  from an analysis of pion electro-production data [7] and direct measurements of the reaction  $p\nu_\mu \rightarrow n\mu^+$  [8].

Of the four f.f.'s, the induced pseudoscalar  $G_{PS}(q^2)$  is the least known. The MuCap collaboration at PSI has recently reported a precise measurement of the rate for capture on hydrogen in the  $1S$  singlet hyperfine state:  $\Gamma(^1\text{H})|_{\text{singlet}} = 725.0 \pm 13.7(\text{stat}) \pm 10.7(\text{syst}) \text{ sec}^{-1}$  [9]. Based on this value, an indirect ‘‘experimental’’ determination of  $G_{PS}$  at the momentum transfer  $q_0^2 = -0.88 m_\mu^2$  relevant for  $\mu^-$  capture on hydrogen,  $G_{PS}^{\text{EXP}}(q_0^2) = 7.3 \pm 1.2$ , has been obtained by using for the remaining f.f.'s the values discussed above and by evaluating electroweak radiative corrections [10]. The latter lead to a 2.8% increase in the rate on hydrogen, and are crucial for bringing  $G_{PS}^{\text{EXP}}$  within less than  $1\sigma$  of the most recent theoretical prediction,  $G_{PS}^{\text{TH}}(q_0^2) = 8.2 \pm 0.2$  [11], obtained in chiral perturbation theory ( $\chi$ PT). For a recent and comprehensive review of theoretical and experimental efforts to determine  $G_{PS}(q^2)$  see Refs. [12, 13].

In the present letter, we focus on the reactions  $^2\text{H}(\mu^-, \nu_\mu)nn$  and  $^3\text{He}(\mu^-, \nu_\mu)^3\text{H}$ , hereafter referred to as  $\mu$ -2 and  $\mu$ -3, respectively. There are a couple of reasons for undertaking this study now: (i) the forthcoming measurement of the  $\mu$ -2 rate  $\Gamma(^2\text{H})$  in the doublet hyperfine state by the MuSun collaboration at PSI with a projected 1% precision [13, 14]. This and the already available, and remarkably precise, measurement of the  $\mu$ -3 rate,  $\Gamma(^3\text{He}) = 1496 \pm 4 \text{ sec}^{-1}$  [15], will make it possible to put tight constraints on  $G_{PS}^{\text{EXP}}(q^2)$  and to test the  $\chi$ PT prediction for this f.f. far more sharply than up to now. (ii) A number of low-energy weak processes of astrophysical interest, such as the weak captures on proton

and  ${}^3\text{He}$ , and neutrino reactions on light nuclei, are not accessible experimentally. In order to have some level of confidence in the reliability of their cross section estimates, it becomes crucial to study, within the same theoretical framework, related electroweak reactions, whose rates are known experimentally, like muon captures [16].

Theoretical work on the  $\mu$ -2 and  $\mu$ -3 reactions is quite extensive (see Refs. [12, 13, 17, 18]). So far, calculations have been performed within two different schemes: the “standard nuclear physics approach” (SNPA) and the approach known as “hybrid” chiral effective field theory ( $\chi$ EFT). In SNPA, Hamiltonians based on conventional two-nucleon (NN) and three-nucleon (NNN) potentials are used to calculate the nuclear w.f.’s, and the weak transition operator includes, beyond the one-body contribution (the impulse approximation—IA) associated with the basic process  $p\mu^- \rightarrow n\nu_\mu$ , meson-exchange currents as well as currents arising from the excitation of  $\Delta$ -isobar degrees of freedom [19]. In the hybrid  $\chi$ EFT approach, the weak operators are derived in  $\chi$ EFT, but their matrix elements are evaluated between w.f.’s obtained from conventional potentials. Typically, the SNPA and hybrid  $\chi$ EFT predictions are in good agreement with each other. For example, for the  $\mu$ -2 rate, the SNPA calculation of Ref. [18] gives  $391 \text{ sec}^{-1}$ , to be compared with the hybrid  $\chi$ EFT studies of Refs. [20] and [18], which report  $386 \text{ sec}^{-1}$  and  $393 \pm 1 \text{ sec}^{-1}$ , respectively. The differences between Refs. [20] and [18] are due to contributions of loop corrections and contact terms in the vector part of the weak current, which were neglected in Ref. [20]. For the  $\mu$ -3 rate, the SNPA calculation of Ref. [18] gives  $1486 \text{ sec}^{-1}$ , while the hybrid  $\chi$ EFT studies of Refs. [21] and [18] report, respectively,  $1499 \pm 16 \text{ sec}^{-1}$  and  $1484 \pm 4 \text{ sec}^{-1}$ . Here, the differences between Refs. [21] and [18] arise mostly from the inclusion in Ref. [21] of vacuum polarization effects on the muon bound state w.f. [10]—these would increase the SNPA and hybrid  $\chi$ EFT results of Ref. [18] quoted above for the  $\mu$ -3 rate to, respectively,  $1496 \text{ sec}^{-1}$  and  $1494 \pm 4 \text{ sec}^{-1}$ .

One of the objectives of the present work is to carry out a  $\chi$ EFT calculation of the  $\mu$ -2 and  $\mu$ -3 rates. Chiral EFT is a formulation of quantum chromodynamics (QCD) in terms of effective degrees of freedom suitable for low-energy nuclear physics: pions and nucleons. The symmetries of QCD, in particular its (spontaneously broken) chiral symmetry, severely restrict the form of the interactions of nucleons and pions among themselves and with external electroweak fields, and make it possible to expand the Lagrangian describing these interactions in powers of  $Q/\Lambda_\chi$ , where  $Q$  is pion momentum and  $\Lambda_\chi \sim 700 \text{ MeV}$  is the chiral-symmetry-breaking scale. As a consequence, classes of Lagrangians emerge, each characterized by a given power of  $Q/\Lambda_\chi$  and each involving a certain number of unknown coefficients, so called low-energy constants (LEC’s). While these LEC’s could in principle be determined by theory (for instance, in lat-

tice QCD calculations), they are in practice constrained by fits to experimental data. Some of them (for example,  $g_A$  and the pion decay amplitude  $F_\pi$ ) characterize the coupling (at lowest order) of pions to nucleons and, in particular, the strength of one- and two-pion-exchange terms (denoted, respectively, OPE and TPE) in the NN potential [22, 23], *i.e.* its long-range components. Some of the other LEC’s multiply NN (and multinucleon) contact interactions, and therefore encode short-range physics, which in a meson-exchange picture would, for example, be associated with vector-meson exchanges or excitation of baryon resonances, like the  $\Delta$  isobar.

The NN potential has been derived up to order  $(Q/\Lambda_\chi)^4$  in the chiral expansion [22, 23]. It consists of OPE and TPE with interaction vertices from leading, next-to-leading, and next-to-next-to-leading  $\pi$ N chiral Lagrangians, and of contact terms. The LEC’s have been constrained by accurate fits to the NN scattering database at energies below the pion production threshold (see Ref. [23] for a review). The NNN potential, which first contributes at order  $(Q/\Lambda_\chi)^3$ , includes  $S$ - and  $P$ -wave TPE—its  $P$ -wave piece is the familiar Fujita-Miyazawa NNN potential—a OPE plus NN contact term with LEC  $c_D$  and a NNN contact terms with LEC  $c_E$ .

The vector and axial pieces of the weak current have been derived up to order  $Q/\Lambda_\chi$  in, respectively, Refs. [24, 25] and [26]. The one-body operators are the same as those obtained in the SNPA by retaining, in the expansion of the covariant single-nucleon four-current, corrections up to order  $(v/c)^2$  relative to the leading-order term [19]. Two-body operators in the axial current (charge) first enter at order  $(Q/\Lambda_\chi)^0$  [ $(Q/\Lambda_\chi)^{-1}$ ], and are suppressed, in the power counting, by  $(Q/\Lambda_\chi)^3$  [ $Q/\Lambda_\chi$ ] relative to the one-body term of order  $(Q/\Lambda_\chi)^{-3}$  [ $(Q/\Lambda_\chi)^{-2}$ ]. In the axial current, these terms include a OPE contribution, involving the known LEC’s  $c_3$  and  $c_4$  (determined by fits to the NN data [23]), and one contact current, whose strength is parametrized by the LEC  $d_R$  (see below). In the axial charge, only OPE contributes, and the associated operator is proportional to  $g_A/F_\pi^2$ . One-loop corrections to the axial charge and current from TPE, which enter at  $Q/\Lambda_\chi$  and are therefore strongly suppressed relative to the leading-order one-body terms, are ignored, since their contributions are expected to be tiny.

The vector weak current is related (via the CVC constraint) to the EM current, which includes, up to order  $Q/\Lambda_\chi$ , OPE and TPE (*i.e.*, one-loop corrections), as well as isoscalar and isovector contact terms, whose strengths are parametrized by the LEC’s denoted, respectively, as  $g_{4S}$  and  $g_{4V}$  in the following [24, 26]. It has been shown [25] that such a current satisfies the continuity equation with the NN potential at order  $(Q/\Lambda_\chi)^2$ . In this regard, we note that the construction of a conserved current with the  $(Q/\Lambda_\chi)^4$  NN potential used here would require the inclusion of terms up to order  $(Q/\Lambda_\chi)^3$ , *i.e.*,

two-loop corrections. This is a daunting task, well beyond the present state of the art. In a more speculative vein, it is also not obvious that such a theory could be made predictive, given the presumably large number of contact terms with unknown LEC's that it would entail.

Finally, we notice that potentials and currents have power-law behavior for large momenta, and need to be regularized. This is accomplished in practice by introducing a momentum-cutoff function. In the present work, the cutoff  $\Lambda$  is taken to be 500 MeV and 600 MeV.

We now turn our attention to the determination of the LEC's  $d_R$ ,  $c_D$ ,  $c_E$ ,  $g_{4S}$ , and  $g_{4V}$ . In the past,  $c_D$  and  $c_E$  were fixed by fitting the triton binding energy (BE) together with an additional strong-interaction observable, such as the  $nd$  doublet scattering length  $^2a_{nd}$  or  $^4\text{He}$  BE. However, this led to significant uncertainties [27]. As the authors of Ref. [28] have observed, the LEC's  $d_R$  and  $c_D$  are related to each other via  $d_R = \frac{M_N}{\Lambda_\chi g_A} c_D + \frac{1}{3} M_N (c_3 + 2c_4) + \frac{1}{6}$  ( $M_N$  is the nucleon mass), and therefore one can fix  $c_D$  (or  $d_R$ ) and  $c_E$  by fitting the triton BE and half-life (specifically, the Gamow-Teller matrix element). Thus, we proceed as follows. The  $^3\text{H}$  and  $^3\text{He}$  ground state w.f.'s are calculated with the hyperspherical-harmonics method (see Ref. [29] for a review) using the chiral NN+NNN potentials of Refs. [22, 23, 30] for  $\Lambda = 500$  and 600 MeV. The corresponding set of LEC's  $\{c_D, c_E\}$  is determined by fitting the  $A = 3$  experimental BE's,  $\text{BE}(^3\text{H})=8.475$  MeV and  $\text{BE}(^3\text{He})=7.725$  MeV, corrected for small contributions (+7 keV in  $^3\text{H}$  and -7 keV in  $^3\text{He}$ ) due to the  $n$ - $p$  mass difference [31], since this effect is neglected in the present calculations. We then span the range  $c_D \in [-3, 3]$ , and, in correspondence to each  $c_D$  in this range, determine  $c_E$  so as to reproduce either  $\text{BE}(^3\text{H})$  or  $\text{BE}(^3\text{He})$ . The resulting trajectories are shown in Fig. 1, and are nearly indistinguishable. Their average, shown by the red lines in Fig. 1, leads to  $A = 3$  BE's within 10 keV of the experimental values above. Then, for each set of  $\{c_D, c_E\}$ , the triton and  $^3\text{He}$  w.f.'s are calculated and, using the  $\chi\text{EFT}$  weak axial current discussed above, the Gamow-Teller matrix element of tritium  $\beta$ -decay ( $\text{GT}^{\text{TH}}$ ) is determined. The ratio  $\text{GT}^{\text{TH}}/\text{GT}^{\text{EXP}}$  is shown in Fig. 2, for both values of the cutoff  $\Lambda$ . We have used  $\text{GT}^{\text{EXP}} = 0.955 \pm 0.004$ , as obtained in Ref. [18], except that we have conservatively doubled the error, represented by the shadowed band in the figure. The range of  $c_D$  values, for which  $\text{GT}^{\text{TH}} = \text{GT}^{\text{EXP}}$  within the experimental error, are  $[-0.20, -0.04]$  for  $\Lambda = 500$  MeV, and  $[-0.32, -0.19]$  for  $\Lambda = 600$  MeV. The corresponding ranges for  $c_E$  are  $[-0.208, -0.184]$  and  $[-0.857, -0.833]$ , respectively. We note that, for each pair of  $\{c_D, c_E\}$  in the selected range, the scattering length  $^2a_{nd}$  is calculated to be  $^2a_{nd} = 0.666 \pm 0.001$  fm for  $\Lambda = 500$  MeV and  $^2a_{nd} = 0.696 \pm 0.001$  fm for  $\Lambda = 600$  MeV, which should be compared with  $^2a_{nd} = 0.675$  fm [29], obtained

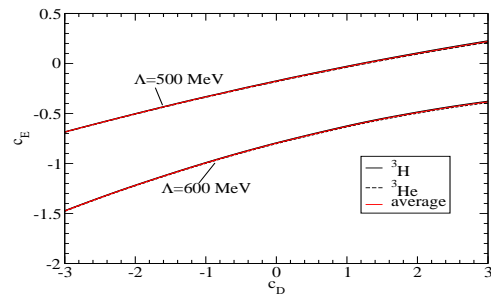


FIG. 1: (Color online)  $c_D$ - $c_E$  trajectories fitted to reproduce the experimental  $^3\text{H}$  and  $^3\text{He}$  BE's. See text for explanation.

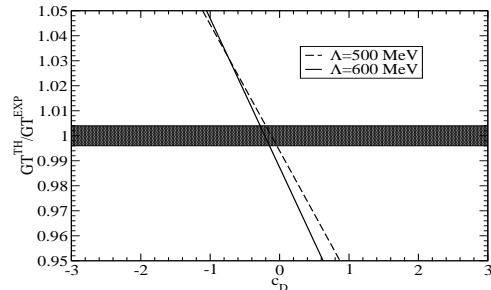


FIG. 2: The ratio  $\text{GT}^{\text{TH}}/\text{GT}^{\text{EXP}}$  as function of the LEC  $c_D$ .

with  $\Lambda = 500$  MeV and  $\{c_D, c_E\} = \{1.0, -0.029\}$ , as originally set in Ref. [30]. The most recent experimental determination gives  $^2a_{nd} = 0.645 \pm 0.010$  fm [32].

For the minimum and maximum values of  $\{c_D, c_E\}$  in the selected range, *i.e.*,  $\{-0.20, -0.208\}$  and  $\{-0.04, -0.184\}$  for  $\Lambda = 500$  MeV, and  $\{-0.32, -0.857\}$  and  $\{-0.19, -0.833\}$  for  $\Lambda = 600$  MeV, we have determined the isoscalar and isovector LEC's,  $g_{4S}$  and  $g_{4V}$ , entering the NN contact terms of the EM current by reproducing the  $A = 3$  magnetic moments. These LEC's are listed in Table I.

TABLE I: The LEC's  $g_{4S}$  and  $g_{4V}$  associated with the isoscalar and isovector NN contact terms in the EM current for  $\Lambda = 500$  and 600 MeV. See text for explanation.

	$\{c_D, c_E\}$	$g_{4S}$	$g_{4V}$
$\Lambda=500$ MeV	$\{-0.20, -0.208\}$	$0.207 \pm 0.007$	$0.765 \pm 0.004$
	$\{-0.04, -0.184\}$	$0.200 \pm 0.007$	$0.771 \pm 0.004$
$\Lambda=600$ MeV	$\{-0.32, -0.857\}$	$0.146 \pm 0.008$	$0.585 \pm 0.004$
	$\{-0.19, -0.833\}$	$0.145 \pm 0.008$	$0.590 \pm 0.004$

Having fully constrained the NNN potential and weak current, we present in Table II the  $\chi\text{EFT}$  predictions for the  $\mu$ -2 and  $\mu$ -3 rates,  $\Gamma(^2\text{H})$  and  $\Gamma(^3\text{He})$ . For  $\Gamma(^2\text{H})$ , we also show the individual contributions of  $nn$  channels with total angular momentum  $J \leq 2$  ( $^1S_0$ ,  $^3P_0$ ,  $^3P_1$ ,  $^3P_2$ ,  $^1D_2$  and  $^3F_2$ ). Higher partial waves are known to contribute less than 0.5 % to  $\Gamma(^2\text{H})$  [18]. The one-body (IA) and (one+two)-body (FULL) results are listed sep-

arately. Note that the IA results depend on the cutoff  $\Lambda$  through the nuclear potentials. Theoretical errors in the FULL results arise from the fitting procedure, and are due primarily to the experimental error on  $\text{GT}^{\text{EXP}}$ . They are not indicated when less than  $0.1 \text{ sec}^{-1}$ . Electroweak radiative corrections have been included as estimated in Ref. [10] for hydrogen and  $^3\text{He}$ —we have assumed that those for deuterium are the same as for hydrogen. The cutoff dependence of the predictions is weak, at less than 1% level, thus suggesting that the mismatch between the chiral order of the potentials and that of the currents may be of little numerical import. If we also account for uncertainties in the electroweak radiative corrections

of the order of 0.4% [10], we can conservatively quote  $\Gamma(^2\text{H}) = 399 \pm 3 \text{ sec}^{-1}$  and  $\Gamma(^3\text{He}) = 1494 \pm 21 \text{ sec}^{-1}$ . These predictions are in good agreement with available experimental data (although those on  $\Gamma(^2\text{H})$  [12] have large errors), as well as with results of recent theoretical studies [18, 20, 21]. Finally, a comparison between the calculated and measured  $\mu$ -3 rates makes it possible to put a constraint on the induced pseudoscalar f.f.  $G_{PS}(q^2)$  at  $q_0^2 = -0.954 m_\mu^2$  relevant for the  $\mu$ -3 reaction. By varying  $G_{PS}(q_0^2)$  so as to match the theoretical upper (lower) value with the experimental lower (upper) value for the rate, we obtain  $G_{PS}(q_0^2) = 8.2 \pm 0.7$ , in good agreement with the  $\chi\text{PT}$  prediction of  $7.99 \pm 0.20$  [11].

TABLE II: Total rates for muon capture on deuteron  $\Gamma(^2\text{H})$  and  $^3\text{He}$   $\Gamma(^3\text{He})$ , in  $\text{sec}^{-1}$ , corresponding to  $\Lambda = 500$  and  $600 \text{ MeV}$ . The one-body (IA) and (one+two)-body (FULL) contributions are listed, along with the individual partial-wave contributions to  $\Gamma(^2\text{H})$ . Theoretical uncertainties in the FULL results, not reported when below  $0.1 \text{ sec}^{-1}$ , are due to the fitting procedure.

	$^1S_0$	$^3P_0$	$^3P_1$	$^3P_2$	$^1D_2$	$^3F_2$	$\Gamma(^2\text{H})$	$\Gamma(^3\text{He})$
IA( $\Lambda = 500 \text{ MeV}$ )	238.8	21.1	44.0	72.4	4.5	0.9	381.7	1362
IA( $\Lambda = 600 \text{ MeV}$ )	238.7	20.9	43.8	72.0	4.5	0.9	380.8	1360
FULL( $\Lambda = 500 \text{ MeV}$ )	$254.4 \pm 0.9$	20.5	46.8	72.1	4.5	0.9	$399.2 \pm 0.9$	$1488 \pm 9$
FULL( $\Lambda = 600 \text{ MeV}$ )	$255.2 \pm 1.0$	20.3	46.6	71.6	4.5	0.9	$399.1 \pm 1.0$	$1499 \pm 9$

The authors would like to thank P. Kammel for encouraging us to carry out this study, and D. Gazit, P. Navrátil and S. Quaglioni for useful discussions. The work of R.S. is supported by the U.S. Department of Energy, Office of Nuclear Physics under contract DE-AC05-06OR23177.

[1] A. Czarnecki, G.P. Lepage, and W.J. Marciano, Phys. Rev. D **61**, 073001 (2000).  
[2] H. Primakoff, Rev. Mod. Phys. **31**, 802 (1959).  
[3] S. Weinberg, Phys. Rev. **112**, 1375 (1958).  
[4] N. Severijns, M. Beck, and O. Naviliat-Cuncic, Rev. Mod. Phys. **78**, 991 (2006).  
[5] C.E. Hyde-Wright and K. de Jager, Ann. Rev. Nucl. Part. Sci. **54**, 217 (2004).  
[6] C. Amsler *et al.* (Particle Data Group), Phys. Lett. B **667**, 1 (2008).  
[7] E. Amaldi, S. Fubini, and G. Furlan, *Electroproduction at Low Energy and Hadron Form Factors*, (Springer Tracts in Modern Physics No. 83, 1979), p.1.  
[8] T. Kitagaki *et al.*, Phys. Rev. D **28**, 436 (1983).  
[9] V.A. Andreev *et al.* (MuCap Collaboration), Phys. Rev. Lett. **99**, 032002 (2007).  
[10] A. Czarnecki, W.J. Marciano, and A. Sirlin, Phys. Rev. Lett. **99**, 032003 (2007).  
[11] V. Bernard, N. Kaiser, and Ulf-G. Meissner, Phys. Rev. D **50**, 6899 (1994); N. Kaiser, Phys. Rev. C **67**, 027002 (2003).  
[12] T. Gorringer and H.W. Fearing, Rev. Mod. Phys. **76**, 31

(2004).  
[13] P. Kammel and K. Kubodera, Ann. Rev. Nucl. Part. Sci. **60**, 327 (2010).  
[14] V.A. Andreev *et al.* (MuSun Collaboration), arXiv:1004.1754.  
[15] P. Ackerbauer *et al.*, Phys. Lett. B **417**, 224 (1998).  
[16] E.G. Adelberger *et al.*, Rev. Mod. Phys. **83**, 195 (2011).  
[17] D.F. Measday, Phys. Rep. **354**, 243 (2001).  
[18] L.E. Marcucci *et al.*, Phys. Rev. C **83**, 014002 (2011).  
[19] L.E. Marcucci *et al.*, Phys. Rev. C **63**, 015801 (2000).  
[20] S. Ando *et al.*, Phys. Lett. B **533**, 25 (2002).  
[21] D. Gazit, Phys. Lett. B **666**, 472 (2008).  
[22] D.R. Entem and R. Machleidt, Phys. Rev. C **68**, 041001 (2003).  
[23] R. Machleidt and D.R. Entem, Phys. Rep. **503**, 1 (2011).  
[24] T.-S. Park, D.-P. Min, and M. Rho, Nucl. Phys. A **596**, 515 (1996); Y.-H. Song, R. Lazauskas, and T.-S. Park, Phys. Rev. C **79**, 064002 (2009).  
[25] S. Pastore *et al.*, Phys. Rev. C **80**, 034004 (2009); S. Kölling *et al.*, Phys. Rev. C **80**, 045502 (2009).  
[26] T.-S. Park *et al.*, Phys. Rev. C **67**, 055206 (2003).  
[27] A. Kievsky *et al.*, Phys. Rev. C **81**, 044003 (2010).  
[28] A. Gardestig and D.R. Phillips, Phys. Rev. Lett. **96**, 232301 (2006); D. Gazit, S. Quaglioni, and P. Navrátil, Phys. Rev. Lett. **103**, 102502 (2009).  
[29] A. Kievsky *et al.*, J. Phys. G: Nucl. Part. Phys. **35**, 063101 (2008).  
[30] P. Navrátil, Few-Body Syst. **41**, 117 (2007).  
[31] A. Nogga *et al.*, Phys. Rev. C **67**, 034004 (2003).  
[32] K. Schoen *et al.*, Phys. Rev. C **67**, 044005 (2003).